Journal of the Geological Society, London, Vol. **170**, 2013, pp. 249–262. doi: 10.1144/jgs2012-029.

The Cretaceous–Tertiary boundary (KTB) transition in NE Brazil

B. GERTSCH[1*], G. KELLER[2], T. ADATTE[3] & Z. BERNER[4]

[1]*Earth, Atmospheric and Planetary Sciences Department, MIT, 77 Massachusetts Avenue, Cambridge, MA 02142, USA*

[2]*Department of Geosciences, Princeton University, Princeton, NJ 08544, USA*

[3]*Institut de Géologie et Paléontologie, Université de Lausanne, Anthropole, CH-1015 Lausanne, Switzerland*

[4]*Karlsruhe Institute of Technology, University, 76131 Karlsruhe, Germany*

**Corresponding author (e-mail: bgertsch@mit.edu)*

Abstract: At 7800 km from Yucatan the Cretaceous–Tertiary boundary (KTB) transition of the Poty Quarry, NE Brazil, is the most distant locality with published accounts of Chicxulub impact–tsunami deposits, impact spherules and Ir anomaly. New investigations based on sedimentology, biostratigraphy, mineralogy and geochemistry fail to confirm these reports. Latest Maastrichtian planktic foraminiferal zones CF1 below an erosive and bioturbated disconformity and early Danian zone P1a(1) above indicate a short hiatus, with the KTB clay (zone P0), the Ir anomaly and the characteristic negative $\delta^{13}C$ excursion missing. The disconformity coincides with the globally recognized latest Maastrichtian sea-level fall. Above the disconformity, an upward-fining micro-conglomerate with abundant reworked Cretaceous foraminifera, sub-angular phosphate clasts, calcitic and phosphatic spheroids along with an early Danian zone P1a(1) assemblage is interpreted as a gravity-flow deposit. Common spheroids throughout the late Campanian–Maastrichtian appear to be chamber infillings of the benthic foraminifer *Dentalina alternata*. Minor Ir anomalies in thin clay layers of zone Pla and no evidence of the Chicxulub impact reveal that the Poty Quarry section remains a very important example of the complex global environmental and sea-level changes observed in KT sequences from North America to Central America that are commonly misinterpreted as impact–tsunami events.

Supplementary materials: Data for trace elements are available at www.geolsoc.org.uk/SUP18585.

Cretaceous–Tertiary boundary (KTB) sequences are rare in South America and are best known from the Neuquén Basin of Argentina and the Paraiba Basin of NE Brazil, with the best sections being recovered from the Poty Quarry near Recife. Early studies of the Poty Quarry claimed a remarkably complete KTB transition with a marly limestone breccia, a graded bioclastic packstone with Chicxulub impact spherules and an iridium anomaly in a thin clay layer at the top (Albertão *et al*. 1994; Albertão & Martins 1996; Marini *et al*. 1998). Most of these studies attributed this sequence to the Chicxulub impact on Yucatan, similar to common interpretations in NE Mexico and Central America (reviewed by Smit, 1999). However, recent publications have advocated two extraterrestrial impacts based on the presence of two small Ir concentrations in the early Danian (e.g. Koutsoukos 1998, 2006; Martins *et al*. 2000; Albertão *et al*. 2004, 2008). The marly limestone breccia and the graded spherule-bearing packstone are commonly named together as a Chicxulub impact ejecta- or tsunami-generated deposit (Smit 1999) or event deposit (Schulte *et al*. 2010). These reports placed the Poty Quarry sequence among the most complete KTB sequences and the only one with Chicxulub impact ejecta deposited *c*. 7800 km from the Yucatan impact crater. Other studies of the Poty sequence suggested that the depositional history was related to sea-level changes across the KT transition, but failed to identify the KTB precisely or determine the origin of impact spherules and Ir concentrations (Mabesoone *et al*. 1968; Stinnesbeck & Keller 1995, 1996). Reinvestigation of the Poty Quarry KTB sequence could therefore yield critical impact information at the greatest distance yet observed from the Chicxulub impact crater on Yucatan and reveal the nature and origin of the event deposit, whether impact–tsunami, storm event, slump or sea-level change.

This study is based on exposures and a new (NSF-funded) drill core from the Poty Quarry that permits examination of the depositional history across the KT transition based on multi-proxy studies, including: (1) geochemical analysis, encompassing stable isotopes, and platinum group elements (PGE); (2) energy-dispersive (EDX) spectroscopy to determine the origin and nature of spherules; (3) sedimentology and microfacies characterization to evaluate the nature and depositional origin of the event deposit; (4) clay mineralogy to evaluate the palaeoclimatic evolution; (5) biostratigraphy based on planktic foraminifera to provide age control.

Location and methods

Cretaceous sediments crop out primarily along the South Atlantic coast of NE Brazil, with the best KTB sections in the Poty Quarry and Itamaraca Island, north of Recife (Mabesoone *et al*. 1968; Riccardi 1987; Fig. 1a). Tectonically, this area is part of the Permambuco–Parana–Rio Grande del Norte basin, which extends from Recife (8°S) to Fortaleza (4°S). It consists of several sub-basins filled by terrestrial and marine sediments after the opening of the equatorial and South Atlantic oceans during the Santonian (Senant & Popoff 1991; Darros de Matos 1992; Mabesoone & Alheiros 1993). The Poty marly limestones of the Gramame Formation are of Maastrichtian age, and are topped by alternating limestone and marl–shale layers of the Palaeocene Maria Farinha Formation (Mabesoone & Alheiros 1993).

The Poty Quarry section was easily accessible until the middle 1990s, but when quarrying ceased the quarry filled with water, leaving just the rim exposed. We obtained NSF funds to drill the KTB and Maastrichtian sequence in the Poty Quarry and two other localities, Itamaraca and Olinda, 30 km to the north and south of Poty (Fig. 1a). In the Poty Quarry, four small exposures and two wells (wells A and B) were drilled to obtain overlapping cores (7°40'S, 34°48'W; Fig. 1b). Lithological changes, disconformities, undulating erosional surfaces, burrows, bioturbation and occurrences of

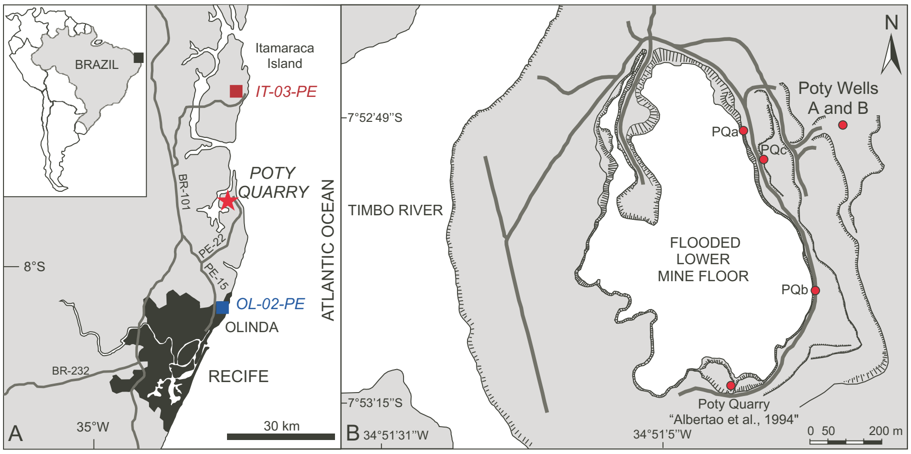

Fig. 1. (**a**) Map of the Recife area with location of the Poty Quarry and wells drilled at Itamaraca, Poty and Olinda in 2005. (**b**) Map of Poty Quarry with the location of the sampled exposures PQa, PQb, PQc, PQ 'Albertao', and Poty Wells-A and -B.

macrofossils were noted, described and photographed for the record. Poty Well-B and the quarry exposures were sampled at 3–5 cm intervals across the suspected KTB and at 5–10 cm intervals through an event deposit (described below), bioturbated intervals and the Danian. The Maastrichtian was sampled at 20 cm intervals. In the laboratory, samples were processed for foraminiferal extraction using standard methods (Keller *et al*. 1995).

The PGE, and carbon and oxygen isotopes were analysed on powdered bulk-rock samples at the Institute for Mineralogy und Geochemistry, Karlsruhe Institute of Technology, Germany. PGE were measured by isotope dilution high-resolution inductively coupled plasma mass spectrometry (HR-ICP-MS) after pre-concentration and matrix reduction by Ni-fire assay (Kramar *et al*. 2001). Carbon and oxygen isotope measurements were carried out using a Delta V Advantage ratio mass spectrometer equipped with an online carbonate preparation line (GasBench) with separate vials for each sample (Thermo Finnigan, Bremen, Germany). The results are expressed on the V-PDB scale with standard deviations <0.05% for $\delta^{13}C$ and <0.1% for $\delta^{18}O$.

Mineralogical analyses were carried out at the Geological Institute of the University of Neuchâtel, Switzerland. Bulk-rock and clay mineral assemblages were analysed by X-ray diffraction (XRD; Scintag XRD 2000 diffractometer) based on procedures described by Kübler 1983) and Adatte *et al*. (1996). This method permits the semi-quantification of whole-rock mineralogy, obtained by XRD patterns of random powder samples by using external standards with a relative error of ±5–10% for the phyllosilicates and 5% for grain minerals. The Calcite/Detritism ratio (C/D = Calcite/(Quartz + Phyllosilicates + Plagioclases + K-Feldspars), an index of detritism, was calculated based on bulk-rock mineralogy to evaluate the variations in detrital input (Adatte *et al*. 2002). The intensities of the identified clay minerals were measured for semi-quantitative estimates of the proportion of clay minerals, which are given in relative per cent without correction factor.

Lithology

Poty Quarry exposures

The limited exposures at the Poty Quarry necessitate a composite of three stratigraphic profiles across the KTB along the quarry lake (PQa, PQb, PQc, Figs 1b and 2a, b). The basal part of this composite section consists of increasingly bioturbated marls and a 2 cm thick clay layer at 1.59 m (1.1–1.75 m). A prominent marly limestone with rare bioturbation marks a sharp lithological change (1.75–2 m). Above these units is a strongly bioturbated marl with large *Thalassinoides* burrows infilled with sub-angular phosphate clasts, glauconite and broken shells in a carbonate matrix (2.0–2.36 m, Fig. 2c). A sharp bioturbated and erosive contact marks a disconformity at the top of this interval. Earlier studies described this bioturbated interval as marly limestone breccia (Albertão *et al*. 1994: Koutsoukos 1998).

Above the disconformity is an event deposit, which is composed of two units separated by an erosion surface. The first unit is an upward fining micro-conglomerate with small sub-angular phosphatic clasts (<5 cm), glauconite grains, and broken shells, including bivalves and gastropods, in a carbonate matrix (2.36–2.6 m, Fig. 2b and d). The second unit above the erosion surface consists of a graded, bioturbated limestone (packstone) with rare, small sub-angular phosphate clasts, glauconite grains and broken shells (2.6–2.75 m; Fig. 2b). These two units have earlier been grouped together and described as bioclastic packstone (Albertão *et al*. 1994; Stinnesbeck & Keller 1996; Koutsoukos 1998). Alternating limestone (mudstone) beds and 2–4 cm thick dark grey marl layers rich in phosphate clasts and glauconite continue through the uppermost part of the section, with the contacts between limestone–marl layers frequently bioturbated (2.75–4.75 m; Fig. 2e).

An additional stratigraphic profile, labelled Poty exposure-2, corresponds to the section described by Albertão *et al*. (1994). This exposure is nowadays flooded, leaving only the event deposit and overlying limestone (mudstone) with dark grey marl layers exposed (Fig. 3a). This interval is similar to the Poty Quarry exposure-1, with an upward-fining micro-conglomerate (0–2 cm), a graded, bioturbated limestone (packstone; 2–15 cm) and alternating dark grey marl and limestone (mudstone) layers (15–30 cm).

Poty Well-B

In the Poty Well-B, the upper Maastrichtian–lower Danian interval reveals the same lithological succession as observed in the exposures (Fig. 3b). The basal part consists of light grey bioturbated marly limestone (15.66–15.28 m), followed by dark grey bioturbated marls (15.28–14.76 m). A burrowed contact marks the transition to bioturbated light-coloured marls with benthic and planktic foraminfera, and rare small phosphate clasts in a fine carbonate matrix (14.76–14.15 m; Fig. 3b, sample 31A). The uppermost part of this interval is strongly bioturbated, with burrows infilled with large sub-angular phosphate clasts, glauconite, shell fragments, secondary pyrite, and benthic and planktic foraminifera in a sparite matrix (14.27–14.15 m). A sharp erosive contact marks the transition to the overlying upward fining micro-conglomerate, which

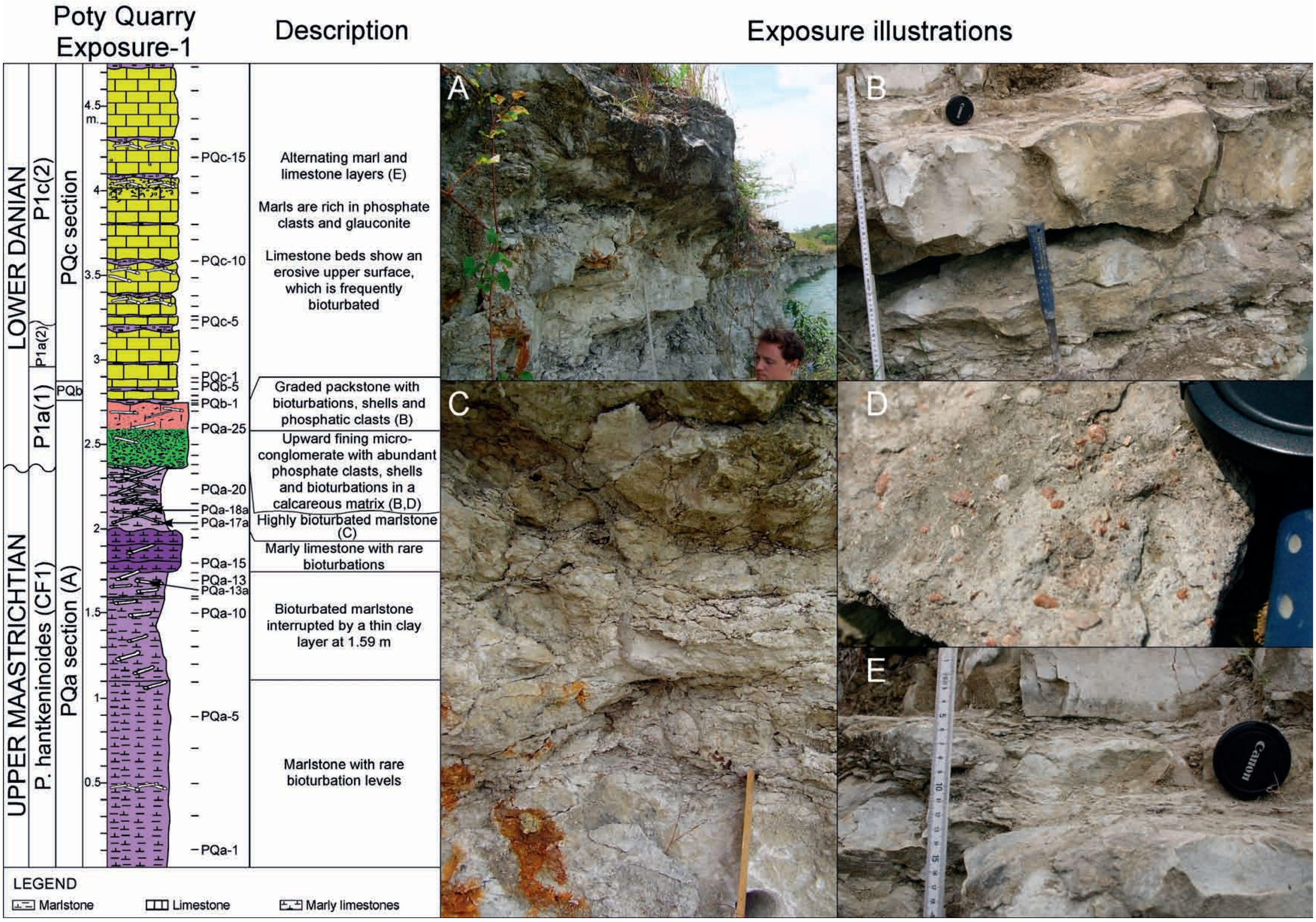

Fig. 2. Lithology of the Poty Quarry exposure-1 with illustrations. (**a**) Outcrop PQa of the Poty Quarry exposure-1. (**b**) Event bed deposit (2.37–2.75 m) composed of an upward-fining micro-conglomerate (2.37–2.6 m) and a graded packstone (2.6–2.75 m). (**c**) Erosive and bioturbated (*Thalassinoides*) contact between strongly bioturbated marlstones and the micro-conglomerate. (**d**) Close-up of phosphate clasts at the base of the micro-conglomerate (2.37–2.59 m). (**e**) Outcrop PQb of the Poty Quarry exposure-1.

consists of large sub-angular phosphatic clasts, glauconite, bivalve shells, and planktic and benthic foraminifera in a carbonate matrix (14.15–13.95 m; Fig. 3b, samples 31C and 31A). Above the erosive contact is an upward fining limestone (packstone) with phosphate clasts and few white and light brown spheroids (<10; 13.93–13.70 m; Fig. 3b, sample 28). This is followed by two thin dark grey marl layers enriched in phosphate clasts, glauconite and shell fragments separated by limestone (mudstone) beds (Fig. 3b, sample 24A, 13.70–13.35 m).

Age and biostratigraphy

The Poty Quarry is the most complete KTB transition in South America, with age control primarily based on planktic foraminiferal biostratigraphy (Albertão *et al*. 1994; Stinnesbeck & Keller 1995; Koutsoukos 1998; Lima & Koutsoukos 2006). Calcareous nannofossils and ostracods are poorly preserved and relatively rare (Stinnesbeck & Reyment 1988; Fauth *et al*. 2005). Planktic foraminifera are abundant, though recrystallized and difficult to free from Cretaceous limestones and marlstones, which prevents quantitative analysis. Therefore, species data are derived from washed residues and thin section analyses. Biostratigraphy is based on the high-resolution Maastrichtian and Danian planktic foraminiferal zonal schemes developed by Keller *et al*. (1995, 2002).

Late Maastrichtian Zone CF1

The total range of *Plummerita hantkeninoides* defines the latest Maastrichtian Zone CF1 (Pardo *et al*. 1996). This biozone spans the upper part of palaeomagnetic chron 29r below the KTB, or about 300 kyr based on the time scale of Cande & Kent (1995) and about 160 kyr based on the time scale of Gradstein & Ogg (2004). This index taxon is commonly present in the Poty Quarry (Figs 4 and 5) and indicates that the uppermost Maastrichtian zone CF1 is present, although truncated by the disconformity at the base of the upward fining micro-conglomerate (Figs 2 and 3a, b). The burrowed interval below the upward fining micro-conglomerate contains only rare poorly preserved and abraded Cretaceous planktic foraminifera that suggest reworking and possibly mixing by burrowing from the upward fining micro-conglomerate above. No Danian species are observed in this interval although their presence in burrows cannot be ruled out (see Koutsoukos 1998).

Late Maastrichtian planktic foraminiferal assemblages are relatively diverse with an average of 25–30 species and a maximum of 42 species (Figs 4 and 5). The lowest number of species is observed in the strongly bioturbated interval below the upward fining micro-conglomerate, where species are rare and show dissolution effects, mechanical abrasion and discoloration similar to the reworked Cretaceous species in the upward fining micro-conglomerate unit. This suggests contamination owing to downward burrowing (Figs 4 and 5).

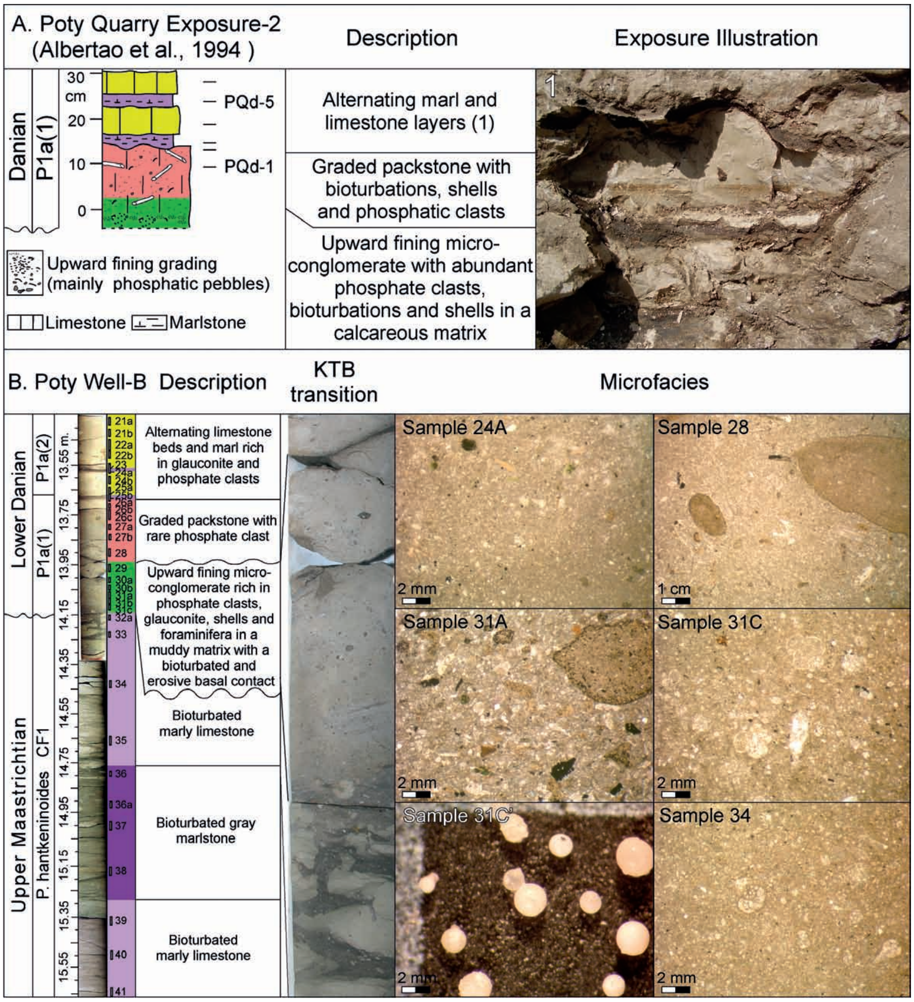

Fig. 3. (**a**) Lithology of the Poty Quarry exposure-2 of Albertão *et al*. (1994). (**b**) Lithological description of Poty Well-B keyed to microfacies. Sample 24A: abundant glauconite and phosphate grains in the thin shale layer. Sample 28: large phosphate clasts in the graded packstone. Sample 31A: abundant phosphate clasts, glauconite and pyrite in the micro-conglomerate. Sample 31C: calcitic spheroids and broken planktic foraminifera in micro-conglomerate. Sample 31C': calcitic spheroids picked from washed residue of the micro-conglomerate. Sample 34: benthic and planktic foraminifera in a fine-grained carbonate matrix of the marly limestone interval.

KT boundary and early Danian

The KT boundary is globally defined by the mass extinction of Maastrichtian planktic foraminifera and the subsequent evolution of the first Danian species *Parvularugoglobigerina extensa, Woodringina hornerstownensis* and *Globoconusa daubjergensis* in the boundary clay zone P0, as observed at El Kef, the Global Stratotype Section and Point (GSSP) and Elles in Tunisia (Keller *et al*. 1995, 2002; Molina *et al*. 2006). Supporting criteria for the KTB definition there include the lithological change at the boundary clay layer with a thin red oxidized layer at the base, an Ir anomaly in the red layer and boundary clay, and a negative $\delta^{13}C$ shift (Cowie *et al*. 1989; Keller *et al*. 1995; Remane *et al*. 1999). Above zone P0 the total range of *Parvularugoglobigerina eugubina* marks zone P1a, which can be subdivided based on the first appearances of *Parasubbotina pseudobulloides* and *Subbotina triloculinoides*).

In the Poty Quarry exposure-1, zone CF1 is truncated at the disconformity below the event deposit. Within the latter, Cretaceous taxa are reworked, as indicated by discoloration, phosphatized shells and clasts, mechanical abrasion, predominance of thick-shelled large species and abundance of robust benthic species. Also present are early Danian species, including *G. daubjergensis, P. extensa, P. eugubina, W. hornerstownensis* and *W. claytonensis*, that indicate deposition of the micro-conglomerate during the early Danian subzone P1a(1) (Figs 4 and 5). These findings are in agreement with earlier studies (e.g. Albertão *et al*. 1994; Koutsoukos 1995, 1998), but not with Stinnesbeck & Keller (1996), who argued against deposition of the micro-conglomerate during the early Danian based on limited sampling.

Koutsoukos (1998) reported the same assemblage plus *Parasubbotina* cf. *pseudobulloides* from the micro-conglomerate as well as the underlying bioturbated marl. His observations suggested that this assemblage is indicative of the upper part of zone P1a (upper Pα of Berggren *et al*. 1995) and tentatively placed the KTB at this level (Koutsoukos 1998). We observed no Danian species in the bioturbated marls, although they may be present in burrows. No typical *P. pseudobulloides* were observed in this study until 27 cm above the micro-conglomerate unit (Figs 4 and 5), which places the KTB at the disconformity at the base of this unit.

Part of the uppermost Maastrichtian zone CF1, the KTB event, zone P0 and most of subzone P1a(1) are missing at this disconformity. The KTB hiatus can be estimated based on sedimentation rates of zones CF1 and P1a. In the Poty Quarry Well-B zone CF1 spans 8 m (Nascimento-Silva *et al*. 2011), and 10 m was reported from another Poty well (Koutsoukos 1998, 2006). Taking the maximum estimate of zone CF1, the sedimentation rate is 6.25 cm a^{-1} based on the time scale of Gradstein & Ogg (2004). This suggests that only about 50 kyr (*c*. 2 m) of zone CF1 are missing. In the early Danian zone P0 and the lower part of subzone P1a(1) are missing, or about *c*. 100–150 kyr. The KTB hiatus therefore spans a relatively short interval with a maximum of *c*. 150–200 kyr.

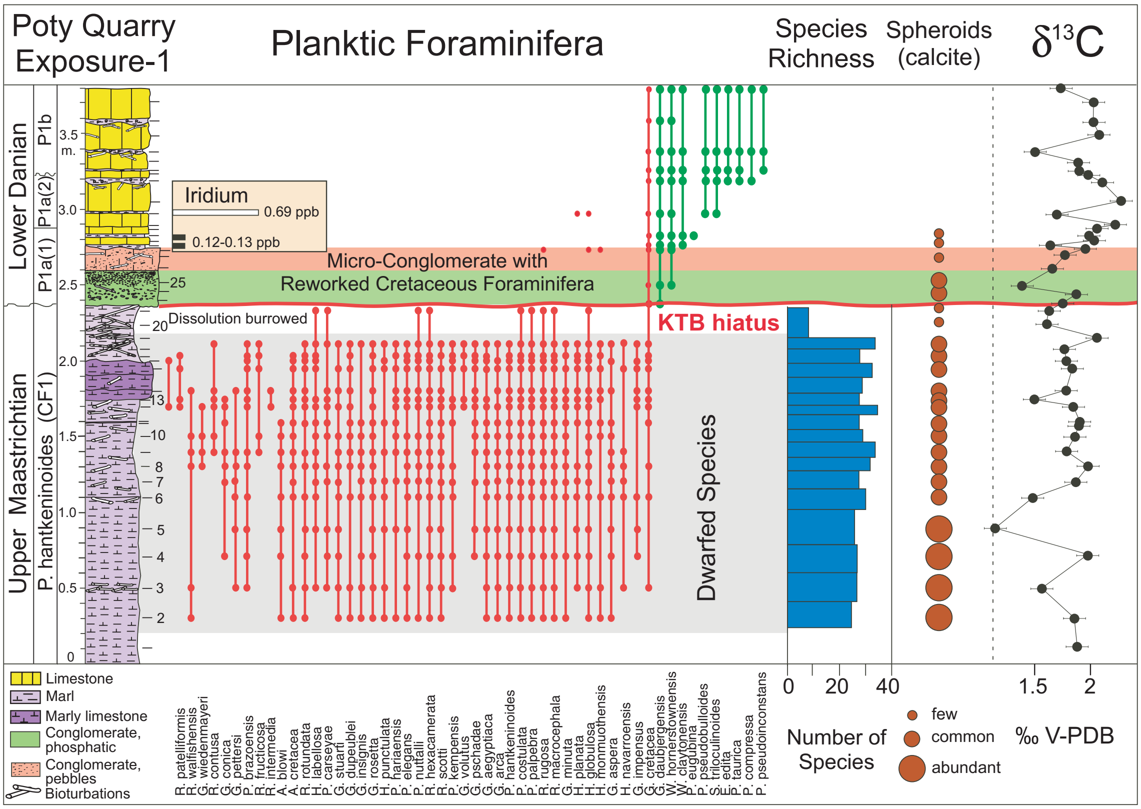

Fig. 4. Late Maastrichtian to early Danian planktic foraminiferal biostratigraphy of Poty Quarry exposure-1, including species ranges, species richness, relative abundance of spheroids, carbon isotopes and Ir concentrations. It should be noted that the largest Ir anomaly (0.69 ppb) was measured by Albertão *et al*. (1994).

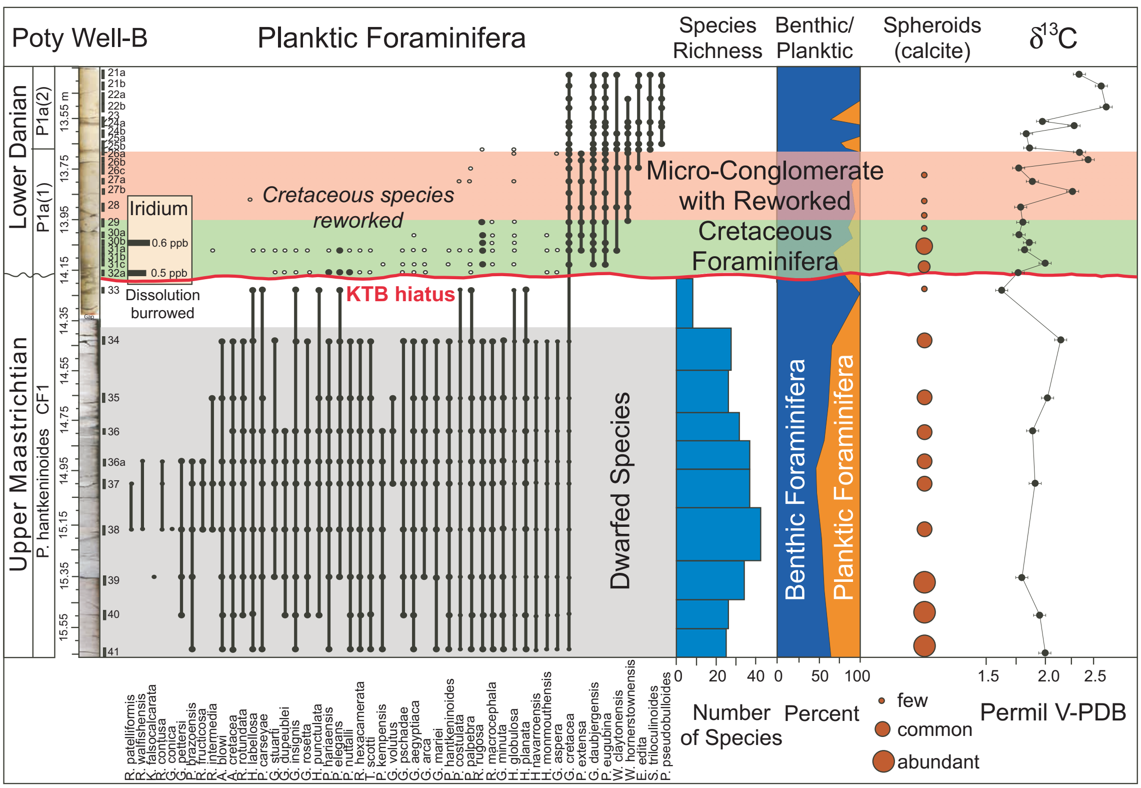

Fig. 5. Late Maastrichtian to early Danian planktic foraminiferal biostratigraphy of Poty Well-B, including species richness, benthic/planktic ratio, relative abundance of spheroids, and carbon isotopes.

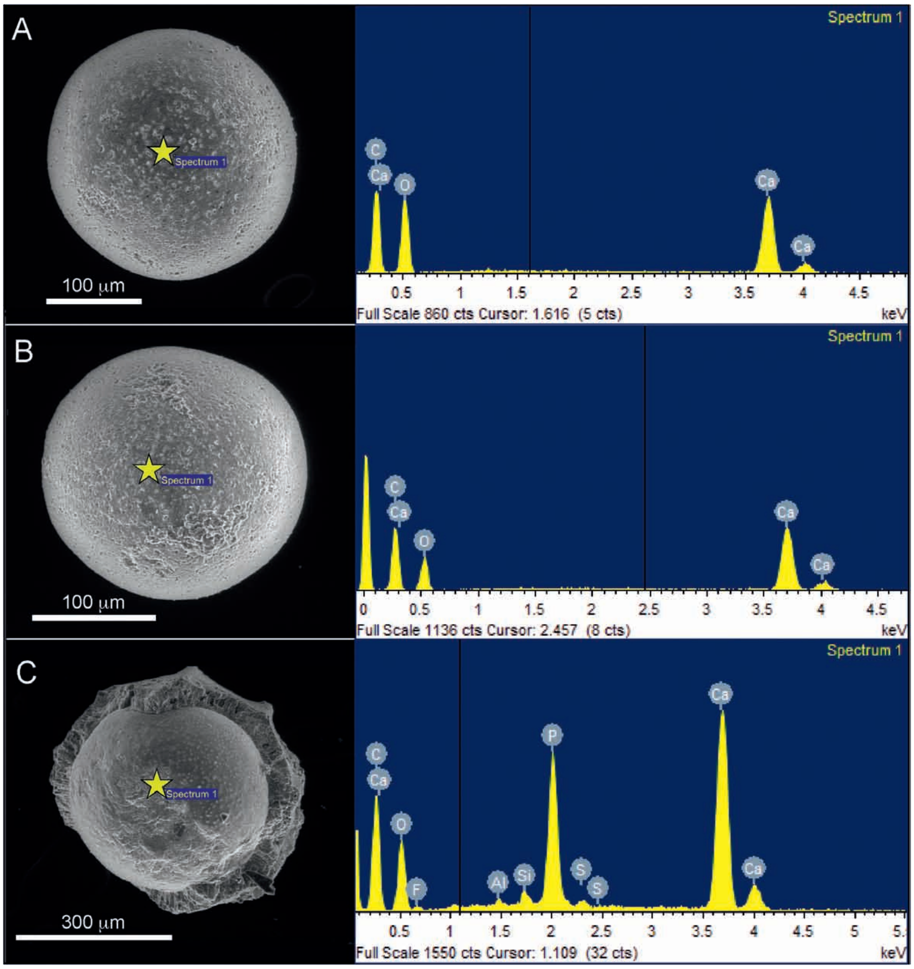

Fig. 6. (**a**, **b**) SEM photographs and EDX spectra of the calcitic spheroids of Poty Well-B. (**c**) SEM photograph and EDX spectra of a phosphatic spheroid from upper Campanian phosphatic limestone at the base of Well-B (CF8b zone).

Spheroids

Spheroids from the Poty Quarry exposure-1 and the Poty Well-B were hand-picked from washed residue of samples. Spheroids are spherical to sub-spherical, with a diameter of 50–300 μm, mostly white and rarely light brown (Fig. 3b). At both sites, abundances of white spheroids decrease in the upper Maastrichtian from abundant (>100) to few (<10) below the KT disconformity (Figs 4 and 5). In the event deposit white and light brown spheroids are mixed and common (10–100) to few (<10) (Figs 4 and 5).

White spheroids with a smooth surface are observed throughout the Maastrichtian and early Danian, and SEM analysis reveals a pure calcitic composition (Fig. 6a–c). The light brown spheroids, frequently surrounded by a brownish crust, are common (10–100) in the late Campanian–early Maastrichtian phosphatic limestone at the base of the Poty Well-B and in the lower Danian event deposit. SEM analysis reveals a Ca–F apatite composition (Fig. 6c).

Stable isotopes

Stable isotopes may be subject to various secondary processes during sediment burial, which can affect carbon and oxygen isotope ratio measurements (Scholle & Arthur 1980; Schrag *et al.* 1995). The effects of allochthonous pore waters and/or recrystallization lead to very negative $\delta^{18}O$ ratios and consequently to significant lowering of the oxygen isotope ratios in sediments (Marshall 1992). In contrast, $\delta^{13}C$ isotopes are little affected by diagenesis, except in sediments influenced by organogenic carbon (Marshall 1992).

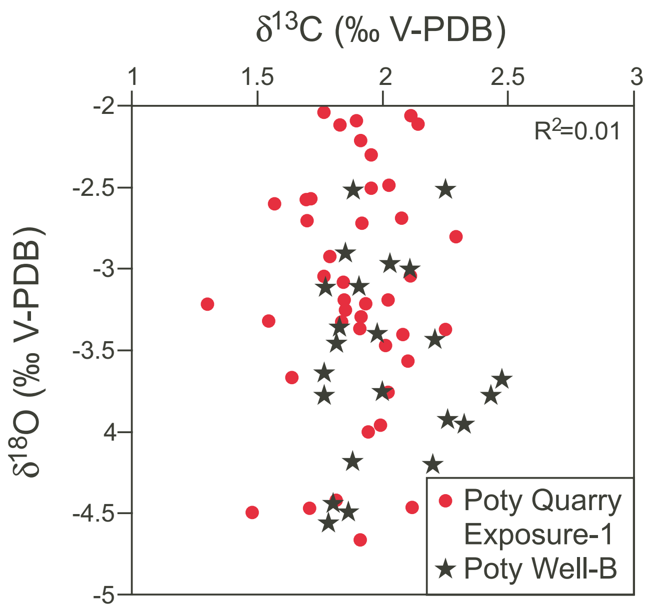

Fig. 7. Cross-plot of the $\delta^{13}C$ and the $\delta^{18}O$ values for Poty Quarry exposure-1 and Poty Well-B. Low correlation factors (R^2) indicate minor diagenetic effects, although rare samples with very low $\delta^{18}O$ values suggest locally high diagenetic effects or insufficient gas from small sample analyses.

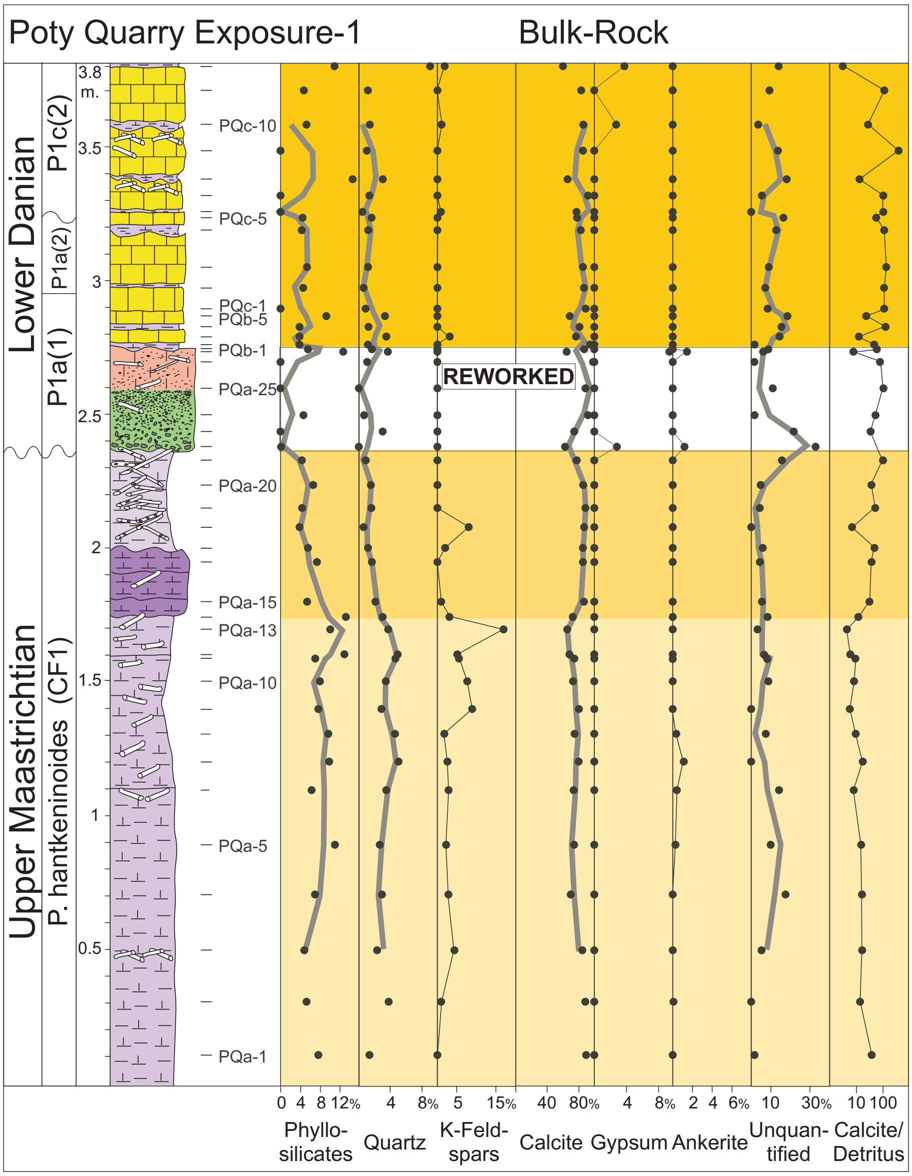

Fig. 8. Bulk-rock analysis of the Poty Quarry exposure-1. Unquantified minerals include a non-identified group of organic material and poorly crystallized minerals. Thick dark grey lines are based on moving averages. (Note the gradual transition from detrital-dominated to carbonate-dominated environments interrupted by a reworked interval in the event deposit.)

In the Poty Quarry exposure-1 and Poty Well-B, diagenetic influence is evaluated by oxygen isotope values (−2.0‰ to −4.8‰) and the cross-plot of δ^{13}C and δ^{18}O (Fig. 7). No correlation is observed ($R^2_{\text{Poty Quarry}}=0.01$; $R^2_{\text{Poty Well-B}}=0.01$), which indicates no strong diagenetic effects linked to the addition of isotopically homogeneous cement affecting both isotopic values (Fig. 7). Given the absence of evidence for preserved or altered organic matter in sediments at Poty (e.g. pyrite), carbon isotope trends are strongly reliable. However, relatively negative δ^{18}O values indicate a diagenetic overprint. In addition, variable lithologies with abrupt contacts across the KT transition and post-depositional stabilization of carbonate matrix to microspar also prevent reliable oxygen isotope interpretations. For these reasons δ^{18}O data are not further discussed.

Carbon isotopes

In the Poty Quarry exposure-1, carbon isotopes display a slight decrease in δ^{13}C values (from 1.9 to 1.6‰) in upper Maastrichtian marls and reach a minimum below the KT disconformity (Fig. 4). Carbon isotope values are not reliable in the reworked sediments of the event deposit (2–2.35 m; Fig. 4). In the alternating Danian limestone and marl layers, δ^{13}C values increase to 2.3‰ and stabilize, but values are low in the marl layers (1.3–1.8‰).

In the Poty Well-B, the carbon isotope curve shows stable values in the upper Maastrichtian zone CF1 (1.9‰), followed by a decrease below the KTB disconformity (1.6‰; Fig. 5). Subzone P1a(1) is marked by stable low δ^{13}C values (1.8‰), except for an isolated peak in the graded packstone (2.2‰). In subzone P1a(2) δ^{13}C values gradually increase (2.4‰), but they display low values in shale layers (1.9‰).

At both sites, the absence of the KTB characteristic 2‰ negative δ^{13}C shift is due to two factors: (1) the disconformity where uppermost Maastrichtian, KTB and lowermost Danian (zone P0 and base of P1a(1)) sediments are missing; (2) the reworked Maastrichtian species in Danian sediments that bias average bulk isotope values.

Mineralogy

Bulk-rock

The Poty Quarry exposure-1 and Poty Well-B mineralogical assemblages are composed mostly of calcite (>75%) with variable, but locally high quartz, phyllosilicates and K-feldspars

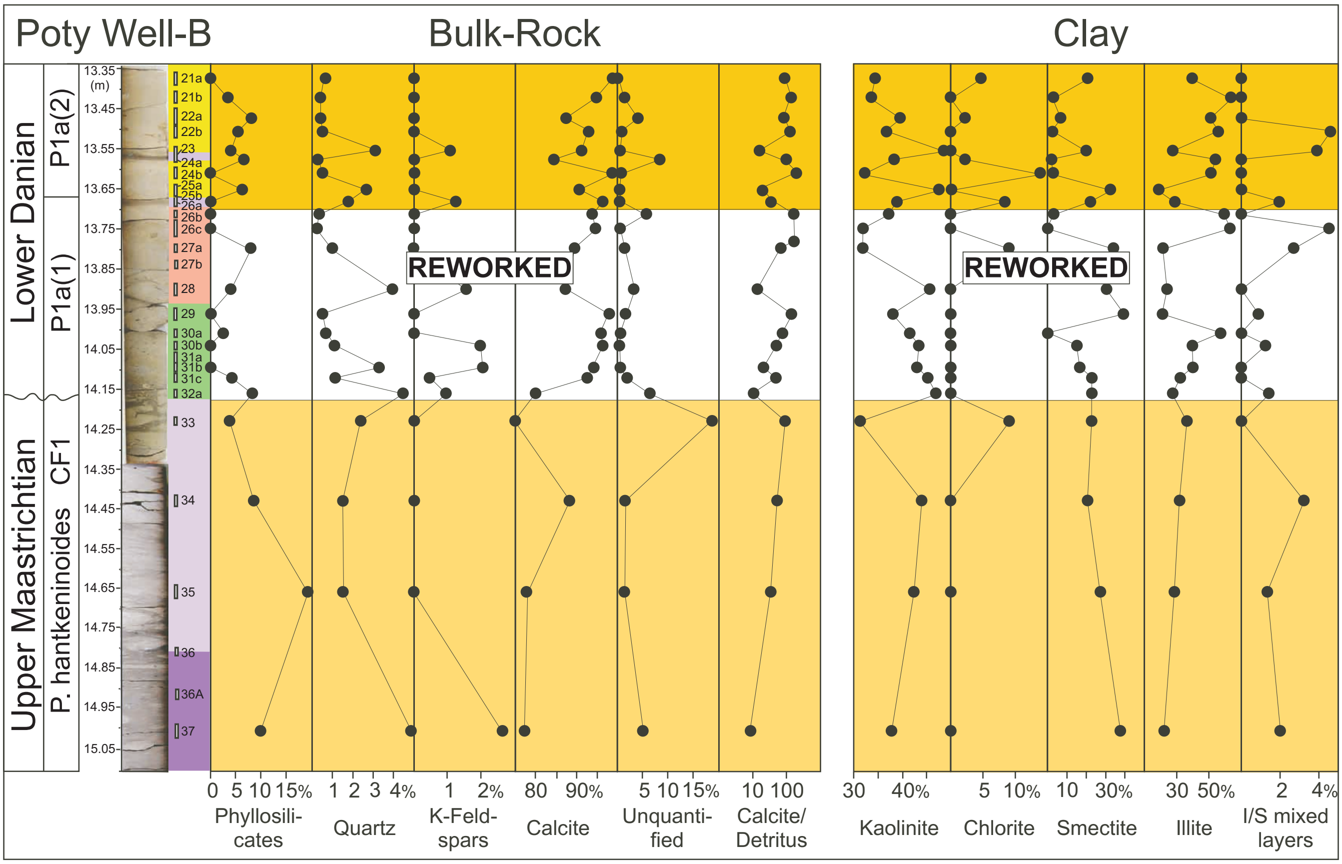

Fig. 9. Mineralogical analysis of bulk-rock and clays of the Poty Well-B. Unquantified minerals include a non-identified group of organic material and poorly crystallized minerals. (Note the gradual transition from detrital-dominated to carbonate-dominated environments interrupted by a reworked interval in the event deposit.)

(Figs 8 and 9). Gypsum and ankerite represent secondary precipitated minerals. Unquantified minerals might consist either of organic matter or poorly crystallized phyllosilicates or phosphate-rich minerals, or a mixing of all the above.

In the Poty Quarry exposure-1, the lower part of the section consists of high but upward-decreasing calcite contents (75–90%), as well as increasing detrital minerals (e.g. phyllosilicates, quartz and K-feldspars (0–1.75 m)). In the middle part of the section, calcite content returns to stable high values (1.75–3.2 m), except for a minor drop in calcite (75%) at the base of the micro-conglomerate above the KTB disconformity. Quartz (2–4%), phyllosilicates (4–8%) and unquantified minerals of phosphate origin (30%) show isolated peaks in the micro-conglomerate (Fig. 8). In the overlying alternating marls and limestone layers calcite dominates and varies with lithological changes (90% in limestone, 70–75% in marly intervals; 3.2–4.75 m). Local high concentrations in phyllosilicates, quartz and K-feldspars are observed in marl layers. The C/D ratios reflect similar trends with decreasing values in the lower part of the section (20–50; 0–1.76 m), followed by high ratios across the KTB disconformity (100, Fig. 8). C/D ratios are high and fluctuating in the alternating marl and limestone (3.2–4.75 m).

In the Poty Well-B, the upper Maastrichtian CF1 zone is composed of calcite (75–85%) and phyllosilicates (5–19%, 15.1–14.25 m, Fig. 9). High unquantified mineral values (18%) are recorded in the strongly bioturbated interval in the uppermost Maastrichtian and related to the abundant phosphate clasts (14.25–14.15 m). The upward fining micro-conglomerate above the KT disconformity records a sudden increase in calcite (90%), near absence of phyllosilicates, and scattered peaks of quartz (4.5%) and K-feldspars (2%, 14.15–13.90 m). Calcite values drop at the base of the graded packstone and gradually increase, whereas detrital minerals (quartz, phyllosilicates and K-feldspars) record scattered peaks (13.90–13.70 m). In the alternating marl and limestone intervals, high calcite contents (85–99%) prevail, but detrital minerals record high values (15%) in marl intervals (13.70–13.35 m). The C/D ratios show upward-increasing values in the upper Maastrichtian CF1 zone (10–100), which are interrupted by a sharp decrease at the KTB disconformity and followed by a gradual increase in the micro-conglomerate (100, 14.15–13.95 m). The contact with the overlying graded packstone marks an abrupt drop in C/D ratios followed by gradually higher values (150, 13.95–13.73 m). In the alternating marls and limestone, C/D ratios are high, except in marl intervals (13.73–13.35 m).

Clay minerals

In Poty Well-B, clay assemblages are dominated by kaolinite, illite and smectite (Fig. 9). Chlorite and illite–smectite (I–S) mixed layers record scattered low peak values at specific levels. The upper Maastrichtian zone CF1 records constant contents of kaolinite (30–45%), smectite (20–30%) and illite (30%; 15.10–14.15 m). A peak in kaolinite (48%) marks the KTB disconformity followed by decreasing values (38%) in the micro-conglomerate. Illite content shows a peak (58%) in the middle of this interval and smectite increases (40%) near the top of the micro-conglomerate (14.15–13.93 m). In the overlying graded packstone, kaolinite increases

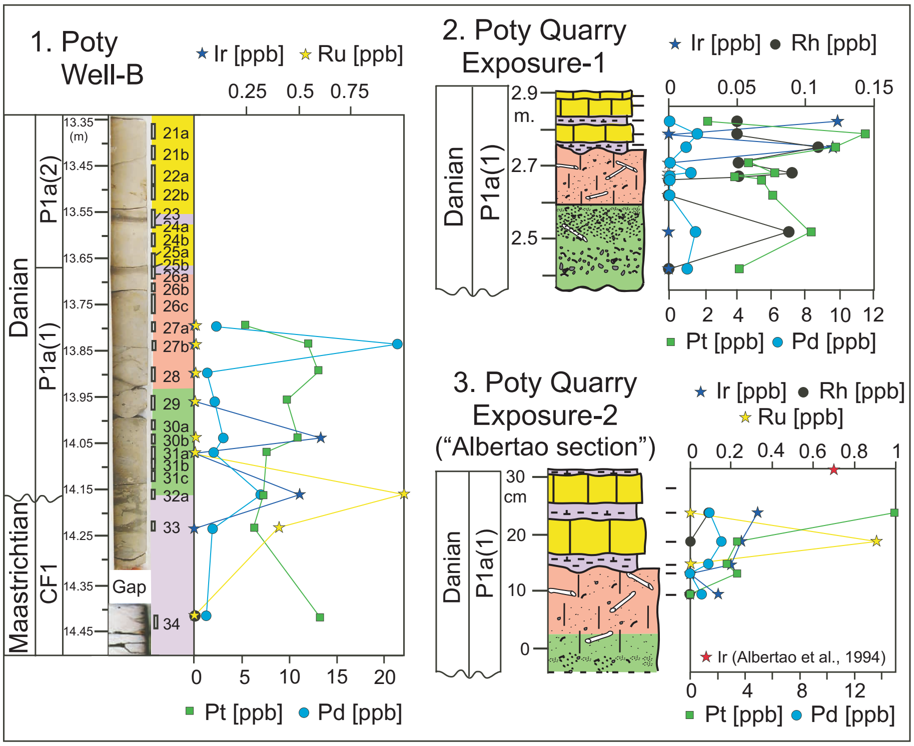

Fig. 10. Platinum group elements (PGE) of the Poty Well-B and Poty Quarry exposures-1 and -2 (Albertao *et al.* 1994). No correlation is observed between the PGE enrichments of these locations.

abruptly at the base (47%) and gradually decreases (32%, 13.93–13.73 m). The top of the graded packstone (65%) is characterized by high illite values (65%) and the disappearance of smectite. In the alternating limestone and marly intervals, limestone beds show high illite contents (50–65%) and marl layers display peaks in kaolinite (48%) and smectite (respectively 20 and 30%).

Platinum group element (PGE) geochemistry

In the Poty Quarry exposure-1, Ir, Pd, Pt and Rh were measured in a 60 cm interval of subzone P1a(1) (2.37–2.97 m, Fig. 10). Only background Ir concentrations are detected in the event deposit and overlying limestone and marl layers (<0.15 ppb), and Pd (0–1 ppb) and Rh values (<0.11 ppb) are similarly very low. Only Pt concentrations are relatively high in the event deposit (4–8 ppb), and reach peak values in the overlying first marl and limestone layers (respectively 9.5 and 11.5 ppb).

In the Poty Quarry exposure-2, PGE analyses of the two marly layers above the event deposit show relatively low and stable Ir (0–0.35 ppb) and Pd values (<2 ppb, Fig. 10). Ru is nearly absent (<0.1 ppb), except for a single peak in a limestone layer above the clastic unit (0.9 ppb). Pt values are usually low (<4 ppb), but show a single peak in the second marl layer (15 ppb). The poor exposure and discontinuous presence of the thin shale layer provided no reliable PGE values, although Albertão *et al.* (1994) recorded 0.69 ppb of Ir.

In the Poty Well-B, Pd, Pt, Ru and Ir were measured across the KTB disconformity and the clastic unit (Fig. 10). Pd values are low (<3 ppb) except for elevated values in the event deposit (sample 32a, 6.9 ppb; sample 27b, 21.3 ppb). Pt values vary between 5 and 13.2 ppb. Ru displays background concentrations (<0.1 ppb), except for two minor enrichments of 0.35 and 1 ppb in the bioturbated interval below the KTB disconformity. Ir concentrations are at background level (<0.1 ppb) except for two peaks (0.5 and 0.6 ppb) in the micro-conglomerate.

Discussion

Palaeoenvironment

Species richness of Cretaceous planktic foraminifera is a good environmental indicator in shelf environments (Koutsoukos 1998; Keller & Abramovich 2009). Outer shelf to upper slope depths (200–300 m) average 45–50 species, middle shelves (100–150 m) 30–40 species and inner shelves (10–50 m) 15–25 species. In the Poty Quarry exposure-1 and Poty Well-B, a maximum of 42 species were observed, with an average of about 30 species per sample, indicating a middle to outer shelf depositional environment. The absence of deep dwellers in these assemblages (e.g. *Gublerina, Abathomphalus*), and the presence of few thermocline dwellers (e.g. globotruncanids, racemiguembelinids) but common surface (e.g. *Pseudoguembelina, Guembelitria*) and subsurface dwellers (e.g. rugoglobigerinids, pseudotextularids, planoglobulinids) (Abramovich *et al.* 2003) suggest deposition at middle shelf depth (100–200 m). This is in good agreement with the presence of glauconite and *Thalassinoides* burrows (MacEachern & Bann 2008), and with the conclusions of Koutsoukos (1998), who estimated middle to outer shelf depths based on benthic foraminifera.

Nature of calcitic and phosphatic spheroids

Previous studies suggested an extraterrestrial origin for the spheroids in the event deposit at Poty (Albertão & Martins 1996; Koutsoukos 1998; Fig. 11a–c). Consequently, the Poty section provided apparently crucial evidence of the Chicxulub ejecta fallout 7800 km from the impact crater on Yucatan, which amplified the known ejecta radius and presumably the global effects of this impact.

Chicxulub impact spherules are characterized by a SiO_2-rich composition and large air bubbles, which are frequently infilled by calcite (Fig. 11d and e; Koeberl & Sigurdsson 1992; Koeberl 1993; Schulte & Kontny 2005; Schulte *et al.* 2009). With diagenetic alteration of the impact glass into pure cheto smectite (Keller *et al.*

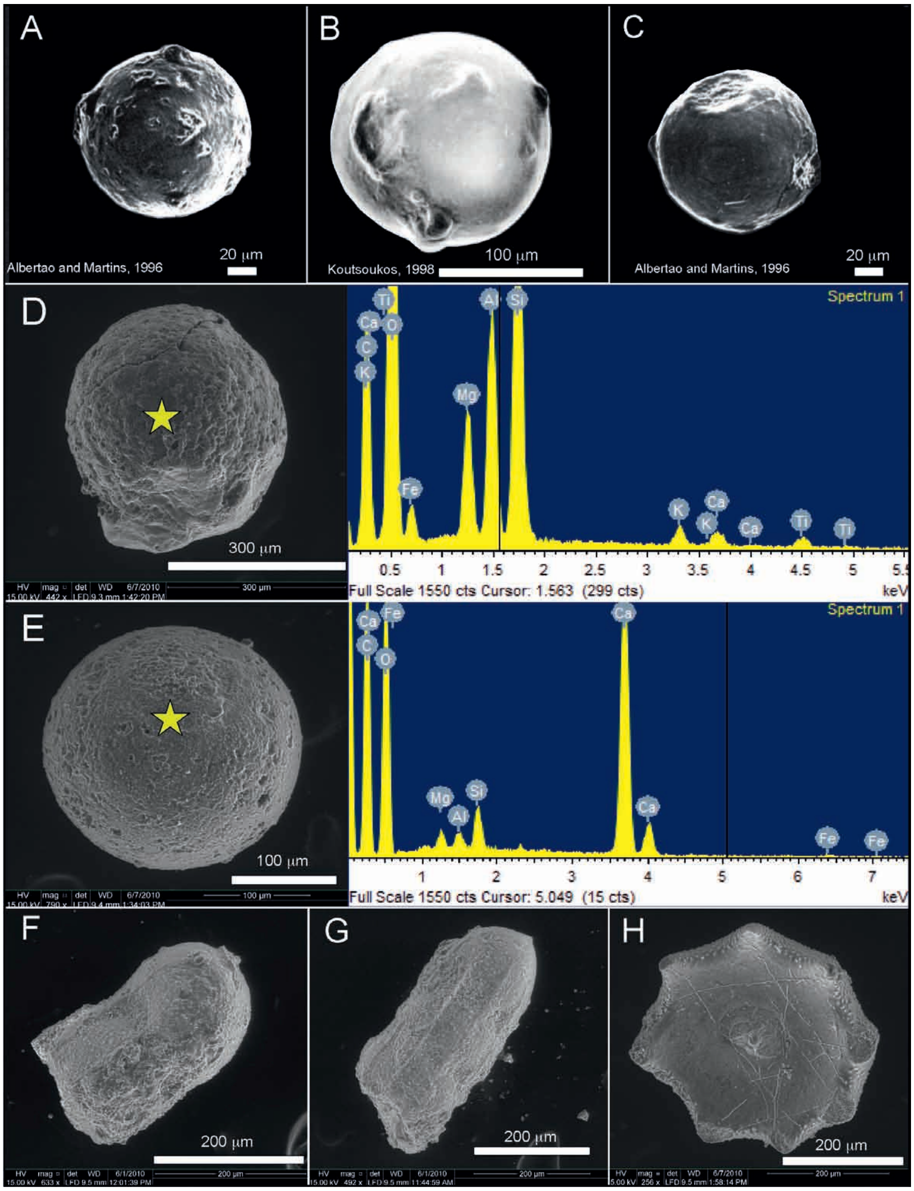

Fig. 11. (**a**–**c**) SEM photographs of the calcitic and phosphatic spherules picked from washed residues of the micro-conglomerate as previously illustrated by Albertão *et al*. (1994, 2004). (**d**) Chicxulub impact spherule from the El Penon section, NE Mexico, and its EDX spectra showing high contents of Al, Si, Mg and Fe. (**e**) Chicxulub impact spherule from Brazos, Texas, and its EDX spectra revealing a calcitic composition and a clay Si–Al-rich coating. (**f**, **g**) Poorly preserved broken shells of Nodosarids. (**h**) Broken phosphatic shell of *Dentalina alternata*, in which calcite infilling resulted in the observed spheroids of Figure 6c.

2003; Adatte *et al*. 2011), the calcite infillings may retain a surface Si–Al coating of the altered impact glass (Berner *et al*. 2007; Ullrich *et al*. 2011). In the Poty Well-B, neither Si–Al-rich surface coating on the calcite spherules nor cheto smectite was detected, except on rare spherules where remnants of clay minerals from the sediment matrix account for the Si–Al coating. The geochemical compositions of the spheroids and their continuous presence during Maastrichtian and Danian intervals do not support an extraterrestrial origin (Figs 4–6).

Alternatively, some of these calcitic and phosphatic spheroids could represent algal resting cysts or calcispheres (pithonellids) with calcite infillings (Stinnesbeck & Keller 1995). Such calcite spheroids are common in the Cretaceous and most abundant in the terminal Maastrichtian (Dias-Brito 2000). In the Poty Quarry, rare to common calcispheres were observed in thin sections, but single hand-picked spheroids from washed residue could not be identified as pithonellids (J. Wendler, pers. comm.).

In this study rare phosphatic spheroids surrounded by an ornamented striated phosphatic crust and common striated shell fragments of the infaunal benthic species *Dentalina alternata* are observed in the late Campanian–early Maastrichtian phosphatic and dolomitic limestone of the Poty Well-B (Fig. 11f–h; Jones 1996; Nascimento-Silva *et al.* 2011). In thin sections, planar cuts of *Dentalina alternata* show the ridge ornaments of the striated shells and the spherical infilling of the foraminiferal chambers. Rare examples of spheroids with adhering shell material can be observed in washed residues. By analogy, the more common white calcite spheroids were probably also derived from foraminiferal chamber infillings. Some white spheroids show protruding mounds as observed by Albertão *et al*. (1994) (Figs 6a, b and 11a–c), which probably correspond to the apertures or connecting siphon between chambers.

Sea-level changes and origin of the event deposit

The Poty Quarry sections are extensively debated owing to the presence of an event deposit near the KTB. These deposits are reminiscent of the siliciclastic deposits in NE Mexico and Texas, which are frequently misinterpreted as being of KTB age and of impact–tsunami

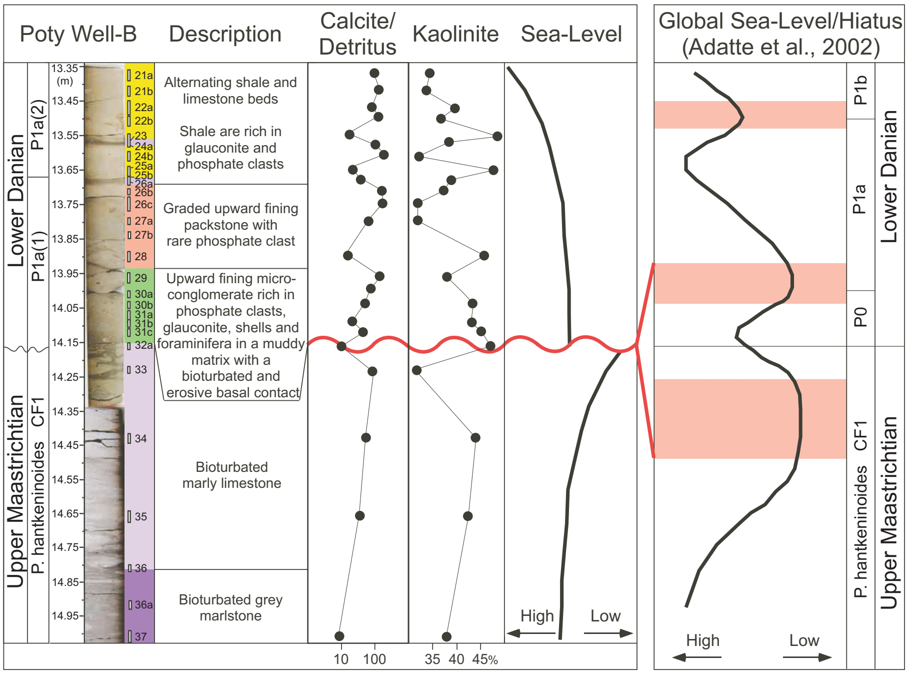

Fig. 12. Sea-level interpretation of the Poty Well-B based on lithological changes, calcite/detritus ratio and kaolinite. These proxies indicate a major sea-level fall in the uppermost Maastrichtian zone CF1 marked by the KTB disconformity. This disconformity is correlative with global sea-level fluctuations and short hiatuses in zone CF1 and the P0–P1a transition.

origin (e.g. Smit 1999; Schulte *et al*. 2010). Others have shown that these deposits are stratigraphically below the KTB and reveal long-term deposition via gravity flows alternating with normal sedimentation during the latest Maastrichtian sea-level fall (Keller *et al*. 2007, 2009*a*, *b*; Adatte *et al*. 2011). This study reveals that the early Danian age of the event deposit at the Poty Quarry and the absence of impact evidence are not compatible with tsunami deposition at the KTB. Sea-level changes and other sedimentary processes must be considered to interpret these Poty sequences.

In the Poty Well-B, sea-level changes can be estimated based on the lithology, C/D index (Li *et al*. 2000; Adatte *et al*. 2002) and kaolinite as indicator of proximality (Adatte *et al*. 1998, 2000; Chamley *et al.* 1989; Fig. 12). In zone CF1 high and increasing C/D ratios suggest a relatively high and stable sea level in an outer to middle shelf environment dominated by carbonate sedimentation. Below the KTB disconformity the decrease in C/D ratios and the peak in kaolinite mark the onset of a sea-level fall in the late Maastrichtian, which culminates at the disconformity that ends Maastrichtian sedimentation (Fig. 12).

After the KT disconformity the overlying upward fining micro-conglomerate with abundant reworked benthic foraminifera, large sub-angular phosphatic clasts and broken shells of bivalves and gastropods suggests erosion and transport from a proximal source. Phosphatic clasts are particularly indicative of erosion because phosphatic deposits are known from only a short interval in the late Campanian of the NE Brazilian shelf (El Gadi & Brookfield 1999; Nascimento-Silva *et al*. 2011). The erosive base of the micro-conglomerate with abundant *Thalassinoides* burrows intruding into the underlying Maastrichtian sediments suggests subaqueous gravity-flow deposition (Grimm & Föllmi 1994). The graded packstone with abundant benthic foraminifera and rare phosphatic clasts indicates a return to a normal sedimentation with a rising sea level in the early Danian (Fig. 12). The mixing of phosphatic and calcitic spheroids in the event deposit reflects reworking and transport from late Campanian phosphatic sediments during a subaqueous concentrated sediment gravity flow. Above the event deposit, a rising sea level is marked by episodes of condensed sedimentation (maximum flooding surface) indicated by high kaolinite and low C/D ratios at the top of the micro-conglomerate and the two thin clay layers (Fig. 12).

Global sea-level falls associated with hiatuses and/or event deposits were previously documented in zones CF1 and early Danian P1(a) (Haq *et al*. 1987; MacLeod & Keller 1991; Stinnesbeck *et al*. 1996; Adatte *et al*. 2002; Keller *et al*. 2009*a*, *b*). In the Pernambuco Basin, a similar KTB disconformity is recorded at Ponte do Funil and in two wells drilled in 2005 at Itamaraca and Olinda (Nascimento-Silva *et al*. 2011). This suggests that both late Maastrichtian CF1 and early Danian P1a(1) sea-level falls are responsible for the KT disconformity on the NE Brazil margin (Fig. 12). The absence of the upward fining micro-conglomerate above the KTB disconformity in some localities (Olinda well, Nascimento-Silva *et al*. 2011) suggests that gravity flows were local.

Nature of the iridium anomaly

The KTB is well known for its global PGE anomalies (e.g. Ir, Pd, Pt, Rh, Ru) commonly recorded in a thin oxidized red clay layer and interpreted as extraterrestrial in origin (Alvarez *et al*. 1980; Frei & Frei 2002; Fornaciari *et al*. 2007). Together with planktic foraminifera, the Ir enrichment at the KTB (although of variable concentrations from 3 to 17 ppb) is a supporting criterion for the definition of the KTB (Keller 2008). At Poty the absence of an Ir anomaly, red clay layer and boundary clay at the KTB disconformity confirms a hiatus (Fig. 10). Multiple PGE peaks appear randomly scattered and cannot be correlated in the Poty sections (Fig. 10). Ir concentrations are small (<0.6 ppb), with a maximum of 0.69 ppb measured in a thin clay layer by Albertão *et al*. (1994) at Poty exposure-2 (Fig. 10). Ir values show two peaks (0.5 and 0.6 ppb) below the KTB disconformity and at the top of the micro-conglomerate in Poty Well-B, but remain below 0.4 ppb in the Poty Quarry exposures-1 and -2.

The small concentrations of Ir (<1 ppb), the absence of correlation between even nearby exposures in the Poty Quarry and occurrence of scattered local enrichments at or close to the lithological contacts prevent a link to an extraterrestrial impact. Recent studies show that Ir anomalies lower than 1 ppb may be caused by concentration during redox fluctuations or sediment starvation (Donovan *et al*. 1988; Colodner *et al*. 1992; Miller *et al*. 2010; Gertsch *et al*. 2011*a*). Redox-sensitive trace elements (Mo, U, V) are related to the presence of phosphate clasts and show no significant variations in the event deposit of the Poty Well-B and Poty Quarry exposure-1. Minor Ir enrichments at Poty are best explained by episodes of sediment starvation at or near maximum flooding surfaces during the early Danian transgression, as observed in similar truncated KT sequences from Central America, Alabama and Texas (Donovan *et al*. 1988; Keller 2008; Gertsch *et al*. 2011*a*).

Palaeoclimatic evolution: clay mineralogy

Clay minerals are formed during the weathering of the continental bedrock and used as climatic proxies (Chamley 1989; Weaver 1989). In proximal marine environments, clay mineral assemblages can indicate sea-level fluctuations depending on the buoyancy of each clay mineral (Chamley 1989; Weaver 1989). At Poty both climatic and sea-level factors need to be taken into account to interpret the clay mineral distribution in these mid- to outer shelf environments.

During the late Maastrichtian, dominant kaolinite suggests warm conditions and abundant rainfall resulting in high continental runoff (Fig. 9; Chamley 1989; Weaver 1989). In the event deposit above the KTB disconformity, scattered clay mineral distribution results from reworked Campanian and Maastrichtian sediments and cannot be used as climate proxy. In the early Danian P1a(2), illite-dominated limestone beds alternate with kaolinite-dominated marls (Fig. 9). Illite indicates overall cooler and drier conditions in the early Danian (Chamley 1989; Weaver 1989). Kaolinite-dominated marls may result from more humid and warmer climate or from lower sea level and more proximal environments, owing to the poor buoyancy of kaolinite (see above). This general climatic pattern, with warm and humid conditions during the late Maastrichtian followed by cooler and drier conditions during the early Danian, agrees with previous palynological and mineralogical studies of the Poty Quarry (Mabesoone *et al*. 1968; Stinnesbeck & Keller 1996) and global climatic trends observed worldwide (Robert & Chamley 1990; Pardo *et al*. 1999; Adatte *et al*. 2002; Gertsch *et al*. 2011*b*).

Depositional scenario and global importance

The depositional history of the KT transition in the Poty Quarry exposures and the Poty Well-B is closely linked to global sea-level variations affecting not only the NE Brazilian margin but also Central America, North Atlantic and Tethys. During the late Maastrichtian zone CF1, carbonate sedimentation in the Poty area occurred in an outer–middle shelf environment (100–150 m). High precipitation and continental runoff during the latest Maastrichtian generated high detrital and nutrient inputs on the shelf. The resulting turbid and mesotrophic marine conditions led to increasingly stratified waters that promoted dwarfed species (e.g. rugoglobigerinids) and opportunistic blooms of *Guembelitria* and *Heterohelix* species.

The latest Maastrichtian sea-level fall coincided with a hiatus of *c*. 150–200 kyr and marked the KTB disconformity. During the subsequent early Danian P1a(1) a gravity flow deposited a micro-conglomerate with a bioturbated and erosive base. Abundant benthic foraminifera, spherical phosphatic and calcitic infillings of chambers (*Dentalina alternata*), broken bivalve and gastropod shells, and phosphatic clasts are indicative of inner shelf environments (70–100 m) and erosion or reworking from a proximal source exposing late Campanian or early Maastrichtian sediments. A rising but fluctuating sea level, drier and colder climatic conditions and reduced continental runoff indicate the return to a middle–outer shelf environment (150–200 m) with reduced biotic stress as evident by increasingly diversified planktic foraminiferal assemblages.

Global sea-level fluctuations during the terminal Maastrichtian–early Danian and/or associated hiatuses are often underestimated in the interpretation of KT sequences. Whereas KT sedimentary successions vary depending on their palaeodepth and geographical and tectonic locations, similar observations noted from the NE Brazilian margin (e.g. KT disconformity and event deposit) are documented also from other inner to middle shelf KT sections of Tunisia and Texas (Adatte *et al*. 2002, 2011). The depositional scenario interpreted from Poty Quarry sequences and the NE Brazilian margin in general recalls the crucial importance of sea-level fluctuations for interpreting sections deposited in inner to outer shelf environments across the KTB.

Conclusions

The investigation of the Poty exposures and Poty Well-B reveals a KT disconformity at the base of a micro-conglomerate bed. The KTB hiatus spans the late CF1 zone to early P1a(1) subzone (*c*. 280 kyr) based on planktic foraminifera. All KTB supporting criteria (e.g. $\delta^{13}C$ shift, Ir anomaly, clay layer) are absent. The KTB disconformity is observed at several sites of the NE Brazilian margin and results from a sea-level fall in the late CF1 Maastrichtian, which correlates with global sea-level trends and hiatus records in Central America and Tethys. In the early Danian a local gravity flow deposited an upward-fining micro-conglomerate with abundant reworked material from proximal environments, followed by a graded packstone indicative of a sea-level transgression.

No impact evidence is present in Poty sequences. Calcitic and phosphatic spheroids are common from early Danian through Maastrichtian to late Campanian sediments and correspond to chamber infillings of the benthic foraminifer *Dentalina alternata* that thrived on the Poty shelf. Rare and small Ir peaks present within the event deposit and in thin shale layers result from sediment starvation under rising sea level that concentrates Ir locally.

We are grateful to J. Hendry, M. Hart and P. Wignall for their thoughtful comments that helped improve this paper. We thank A. Barbosa and V. Neumann for their support during drilling and fieldwork, and G. Poirier, Material Science Department of Princeton University, for assistance with SEM work. We are grateful to A. Villars for preparing the thin sections. Research and continental drilling were supported by the US National Science Foundation (NSF) and OISE Grant No. EAR-0207407 to G.K., and geochemical analyses were partly funded by the Deutsche Forschungsgemeinschaft Grant STU 169/34.

References

Abramovich, S., Keller, G., Stüben, D. & Berner, Z. 2003. Characterization of late Campanian and Maastrichtian planktonic foraminiferal depth habitats and vital activities based on stable isotopes. *Palaeogeography, Palaeoclimatology, Palaeoecology*, **202**, 1–29.

Adatte, T., Stinnesbeck, W. & Keller, G. 1996. Lithostratigraphic and mineralogic correlations of near K/T boundary sediments northeastern Mexico: Implications for origin and nature of deposition. *In*: Ryder, G., Fastovsky, D.E. & Gartner, S. (eds) *The Cretaceous–Tertiary Event and Other Catastrophes in Earth History*. Geological Society of America, Special Papers, **307**, 211–226.

Adatte, T., Keller, G., Li, L., Stinnesbeck, W. & Zaghbib-Turki, D. 1998. Climate and sea level fluctuations across the K–T boundary in Tunisia: Warm and humid conditions linked to the Deccan volcanism? *In*: *International Workshop on Cretaceous–Tertiary Transition (Abstracts)*. Office National des Mines, Direction du Service Géologique, Tunis, 7–10.

Adatte, T., Bolle, M.P., De Kaenel, E., Gawenda, P., Winkler, W. & Von Salis, K. 2000. Climatic evolution from Paleocene to earliest Eocene inferred from clay-mineral: A transect from northern Spain (Zumaya) to southern (Spain, Tunisia) and southern-east Tethys margins (Israel, Negev). *GFF*, **122**, 7–8.

Adatte, T., Keller, G. & Stinnesbeck, W. 2002. Late Cretaceous to early Paleocene climate and sea-level fluctuations: The Tunisian record. *Palaeogeography, Palaeoclimatology, Palaeoecology*, **178**, 165–196.

Adatte, T., Keller, G. & Baum, G.R. 2011. Age and origin of the Chicxulub impact and sandstone complex, Brazos River, Texas: Evidence from lithostratigraphy and sedimentology. *In*: Keller, G. & Adatte, T. (eds) *End-Cretaceous Mass Extinction and the Chicxulub Impact in Texas*. SEPM Special Publications, **100**, 43–80.

Albertão, G.A. & Martins, P.P., Jr. 1996. A possible tsunami deposit at the Cretaceous–Tertiary boundary in Pernambuco, northeastern Brazil. *Sedimentary Geology*, **104**, 189–201.

Albertão, G.A., Koutsoukos, E.A.M., Regali, M.P.S., Attrep, M., Jr. & Martins, P.P., Jr. 1994. The Cretaceous–Tertiary boundary in southern low-latitude regions: preliminary study in Pernambuco, northeastern Brazil. *Terra Nova*, **6**, 366–375.

Albertão, G.A., de Azevedo Grassi, A., Marini, F., Martins, P.P., Jr. & de Ros, L.F. 2004. The K–T boundary in Brazilian marginal sedimentary basins and related spherules. *Geochemical Journal*, **38**, 121–128.

Albertão, G.A., Martins, P.P., Jr. & Marini, F. 2008. Tsunamiites—conceptual descriptions and a possible case at the Cretaceous–Tertiary boundary in the Pernambuco Basin, northeastern Brazil. *In*: Shiki, T., Tsui, Y., Yamazaki, T. & Minoura, K. (eds) *Tsunamiites*. Elsevier, Amsterdam, 217–250.

Alvarez, L.W., Alvarez, W., Asaro, F. & Michel, H.V. 1980. Extraterrestrial cause for the Cretaceous–Tertiary boundary. *Science*, **208**, 1095–1108.

Berggren, W.A., Kent, D.V., Swisher, C.C. & Aubry, M.P. 1995. A revised Cenozoic geochronology and chronostratigraphy. *In*: Berggren, W.A., Kent, D.V., Aubry, M.-P. & Hardenbol, J. (eds) *Geochronology, Time Scales and Stratigraphic Correlation.* SEPM Special Publications, **54**, 129–213.

Berner, Z., Keller, G., Kramar, U., Stueben, D. & Schwotzer, M. 2007. New Ir data from K–T sections in the Paraiba Basin, NE Brazil. *Geochimica et Cosmochimica Acta*, Supplement 15S, **71**, A85.

Cande, S.C. & Kent, D.V. 1995. Revised calibration of the geomagnetic polarity time scale for the late Cretaceous and Cenozoic. *Journal of Geophysical Research*, **100**, 6093–6095.

Chamley, H. 1989. *Clay Sedimentology*. Springer, Berlin, 623pp.

Colodner, D.C., Boyle, E.A., Edmond, J.M. & Thomson, J. 1992. Post-depositional mobility of platinum, iridium, and rhenium in marine sediments. *Nature*, **358**, 402–404.

Cowie, J.W., Ziegler, W. & Remane, J. 1989. Stratigraphic Commission accelerates progress, 1984 to 1989. *Episodes*, **12**, 79–83.

Darros de Matos, R. 1992. The Northeast Brazilian Rift System. *Tectonophysics*, **11**, 766–791.

Dias-Brito, D. 2000. Global stratigraphy, palaeobiogeography and palaeoecology of Albian–Maastrichtian pithonellid calcispheres: Impact on Tethys configuration. *Cretaceous Research*, **21**, 315–349.

Donovan, A.D., Baum, G.R., Blechschmidt, G.L., Loutit, T.S., Pflum, C.E. & Vail, P.R. 1988. Sequence stratigraphic setting of the Cretaceous–Tertiary Boundary in central Alabama. *In*: Wilgus, C.K., Hastings, B.K., Posamentier, H., Van Wagoner, J., Ross, C.A. & Kendall, C.G.St.C. (eds) *Sea-Level Changes—An Integrated Approach*. SEPM Special Publications, **42**, 299–307.

El Gadi, M.S.M. & Brookfield, M.E. 1999. Open carbonate ramp facies, microfacies and paleoenvironments of the Gramame Formation (Maastrichtian), Pernambuco–Paraiba Basin, northeastern Brazil. *Journal of South American Earth Sciences*, **12**, 411–433.

Fauth, G., Colin, J.-P., Koutsoukos, E.A.M. & Bengston, P. 2005. Cretaceous–Tertiary boundary ostracodes from the Poty Quarry, Pernambuco, northeastern Brazil. *Journal of South American Earth Sciences*, **19**, 285–305.

Fornaciari, E., Giusberti, L., *et al*. 2007. An expanded Cretaceous–Tertiary transition in a pelagic setting of the Southern Alps (central–western Tethys). *Palaeogeography, Palaeoclimatology, Palaeoecology*, **255**, 98–131.

Frei, R. & Frei, K.M. 2002. A multi-isotopic and trace element investigation of the Cretaceous–Tertiary boundary layer at Stevns Klint, Denmark—inferences for the origin and nature of siderophile and lithophile element geochemical anomalies. *Earth and Planetary Science Letters*, **203**, 691–708.

Gertsch, B., Keller, G., Adatte, T. & Berner, Z. 2011*a*. Platinum group element (PGE) geochemistry of Brazos sections, Texas, U.S.A. *In*: Keller, G. & Adatte, T. (eds) End-Cretaceous Mass Extinction and the Chicxulub Impact in Texas. SEPM Special Publications, **100**, 227–249.

Gertsch, B., Keller, G., Adatte, T., Garg, R., Prasad, V., Berner, Z. & Fleitmann, D. 2011*b*. Environmental effects of Deccan volcanism across the Cretaceous–Tertiary transition in Meghalaya, India. *Earth and Planetary Science Letters*, **310**, 272–285.

Gradstein, F.M. & Ogg, J.G. 2004. Geologic Time Scale 2004—why, how, and where next! *Lethaia*, **37**, 175–181.

Grimm, K.A. & Föllmi, K.B. 1994. Doomed pioneers: Allochthonous crustacean tracemakers in anaerobic basinal strata, Oligo-Miocene San Gregorio Formation, Baja California Sur, Mexico. *Palaios*, **9**, 313–334.

Haq, B.U., Hardenbol, J. & Vail, P.R. 1987. Chronology of fluctuating sea-levels since the Triassic. *Science*, **235**, 1156–1167.

Jones, R.W. 1996. *Micropaleontology in Petroleum Exploration*. Oxford Science Publications, Oxford.

Keller, G. 2008. Impact stratigraphy: old principle—new reality. *In*: Evans, K.R., Wright Horton Jr, J., King Jr, D.T. & Morrow, J.R. (eds) *The Sedimentary Record of Meteorite Impacts*. Geological Society of America, Special Papers, **437**, 47–72.

Keller, G. & Abramovich, S. 2009. Lilliput effect in late Maastrichtian planktic foraminifera: response to environmental stress. *Palaeogeography, Palaeoclimatology, Palaeoecology*, **284**, 47–62.

Keller, G., Li, L. & MacLeod, N. 1995. The Cretaceous/Tertiary boundary stratotype section at El Kef, Tunisia: How catastrophic was the mass extinction? *Palaeogeography, Palaeoclimatology, Palaeoecology*, **119**, 221–254.

Keller, G., Adatte, T., Burns, S.J. & Tantawy, A. 2002. High stress paleoenvironment during the late Maastrichtian to early Paleocene in Central Egypt. *Paleogeography, Paleoclimatology, Paleoecology*, **187**, 35–60.

Keller, G., Stinnesbeck, W., *et al*. 2003. Spherule deposits in Cretaceous–Tertiary boundary sediments in Belize and Guatemala. *Journal of the Geological Society, London*, **160**, 1–13.

Keller, G., Adatte, T., *et al*. 2007. Chicxulub impact predates K–T boundary: New evidence from Brazos, Texas. *Earth and Planetary Science Letters*, **255**, 339–356.

Keller, G., Abramovich, S., Berner, Z. & Adatte, T. 2009*a*. Biotic effects of the Chicxulub impact, K–T catastrophe and sea-level change in Texas. *Paleogeography, Paleoclimatology, Paleoecology*, **271**, 52–68.

Keller, G., Adatte, T., Pardo Juez, A. & Lopez-Oliva, J.G. 2009*b*. New evidence concerning the age and biotic effects of the Chicxulub impact in NE Mexico. *Journal of the Geological Society, London*, **166**, 393–411.

Koeberl, C. 1993. Chicxulub Crater, Yucatan: tektites, impact glasses, and the geochemistry of target rocks and breccias. *Geology*, **21**, 211–214.

Koeberl, C. & Sigurdsson, H. 1992. Geochemistry of impact glasses from the K/T boundary in Haiti: Relation to smectites and a new type of glass. *Geochimica et Cosmochimica Acta*, **56**, 2113–2129.

Koutsoukos, E.A.M. 1995. Reply to "The Cretaceous–Tertiary boundary in southern low-latitude regions: preliminary study in Pernambuco, northeastern Brazil Comments". *Terra Nova*, **7**, 378–382.

Koutsoukos, E.A.M. 1998. An extraterrestrial impact in the early Danian: A secondary K–T boundary event? *Terra Nova*, **10**, 68–73.

Koutsoukos, E.A.M. 2006. The Cretaceous–Paleogene boundary at the Poty section, NE Brazil: foraminiferal record and sequence of events—a review. *Anuario do Instituto de Geociencias*, **29**, 95–107.

Kramar, U., Stüben, D., Berner, Z., Stinnesbeck, W., Philipp, H. & Keller, G. 2001. Are Ir anomalies sufficient and unique indicators for cosmic events? *Planetary and Space Science*, **49**, 831–837.

Kübler, B. 1983. Dosage quantitative des minéraux majeurs des roches sedimentaires par diffraction X. *Cahiers de l'Institut de Géologie, Neuchâtel, Série ADX*, **1.1–1.2**, 1–13.

Li, L., Keller, G., Adatte, T. & Stinnesbeck, W. 2000. Late Cretaceous sea-level changes in Tunisia: a multi-disciplinary approach. *Journal of the Geological Society, London*, **157**, 447–458.

Lima, F.H.O. & Koutsoukos, E.A.M. 2006. Towards an integrated stratigraphy of the Gramame Formation (Maastrichtian), CIPASA Quarry, Pernambuco–Paraiba Basin, NE Brazil. *Annuario do Instituto de Geociencias*, **29**, 81–94.

Mabesoone, J.M. & Alheiros, M.M. 1993. Evolution of the Pernambuco–Paraiba–Rio Grande do Norte Basin and the problem of the South Atlantic connection. *Geologie en Mijnbouw*, **71**, 351–362.

Mabesoone, J.M., Tinico, I.M. & Coutinho, P.N. 1968. The Mesozoic–Tertiary boundary in Northeastern Brazil. *Palaeogeography, Palaeoclimatology, Palaeecology*, **4**, 161–185.

Maceachern, J.A. & Bann, K.L. 2008. The role of ichnology in refining shallow marine facies models. *In*: Hampson, G.J., Steel, R.J., Burgess, P.M. & Dalrymple, R.W. (eds) *Recent Advances in Models of Siliciclastic Shallow-Marine Stratigraphy*. SEPM Special Publications, **90**, 73–116.

MacLeod, N. & Keller, G. 1991. Hiatus distributions and mass extinctions at the Cretaceous/Tertiary boundary. *Geology*, **19**, 479–501.

Marini, F., Albertão, G.A., Oliveira, A.D. & Delício, M.P. 1998. Preliminary SEM and EPMA investigations on KTB spherules from the Pernambuco area (NE Brazil). *In*: Detre, C.H. & Toth, I. (eds). *Extracts of 1998 Annual Meeting of IGCP 384, Budapest*. 61–62.

Marshall, J.D. 1992. Climatic and oceanographic isotopic signals from the carbonate rock record and their preservation. *Geological Magazine*, **129**, 143–160.

Martins, P.P., Albertao, G.A. & Haddad, R. 2000. The Cretaceous–Tertiary boundary in the context of impact geology and sedimentary record—an analytical review of 10 yrs of researches in Brazil. *Revista Brasileira de Geociencias*, **30**, 460–465.

Miller, K.G., Sherrell, R.M., *et al*. 2010. Relationship between mass extinction and iridium across the Cretaceous–Paleogene boundary in New Jersey. *Geology*, **38**, 867–870.

Molina, E., Alegret, L., *et al*. 2006. The Global Boundary Stratotype Section and Point for the base of the Danian Stage (Paleocene, Paleogene, 'Tertiary', Cenozoic) at El Kef, Tunisia—Original definition and revision. *Episodes*, **29**, 263–273.

Nascimento-Silva, M.V., Sial, A.N., *et al*. 2011. Cretaceous–Paleogene transition at the Paraiba Basin, northeastern Brazil: carbon-isotope and mercury subsurface stratigraphies. *Journal of South American Earth Sciences*, **32**, 379–392.

Pardo, A., Ortiz, N. & Keller, G. 1996. Latest Maastrichtian foraminiferal turnover and its environmental implications at Agost, Spain. *In*: MacLeod, N. & Keller, G. (eds) *Cretaceous/Tertiary Boundary Mass Extinction: Biotic and Environmental Changes*. Norton, New York, 139–172.

Pardo, A., Adatte, T., Keller, G. & Oberhansli, H. 1999. Paleoenvironmental changes across the Cretaceous–Tertiary boundary at Koshak, Kazakhstan, based on planktic foraminifera and clay mineralogy. *Palaeogeography, Palaeoclimatology, Palaeoecology*, **154**, 247–273.

Remane, J., Keller, G., Hardenbol, J. & Ben Haj Ali, M. l999. Report on the International Workshop on Cretaceous–Paleogene Transitions. *Episodes*, **22**, 47–48.

Riccardi, A.C. 1987. Cretaceous paleogeography of southern South America. *Palaeogeography, Palaeclimatology, Palaeoecology*, **59**, 169–195.

Robert, C. & Chamley, H. 1990. Paleoenvironmental significance of clay mineral association at the Cretaceous–Tertiary boundary. *Palaeogeography, Palaeoclimatology, Palaeoecology*, **79**, 205–219.

Scholle, P.A. & Arthur, M.A. 1980. Carbon isotopes fluctuations in Cretaceous pelagic limestones: Potential stratigraphic and petroleum exploration tool. *AAPG Bulletin*, **64**, 67–87.

Schrag, D.P., Depaolo, D.J. & Richter, F.M. 1995. Reconstructing past sea surface temperatures: correcting for diagenesis of bulk marine carbonate. *Geochimica et Cosmochimica Acta*, **59**, 2265–2278.

Schulte, P. & Kontny, A. 2005. Chicxulub impact ejecta from the Cretaceous–Paleogene (K–P) boundary in northeastern Mexico. *In*: Kenkmann, T., Hörz, F. & Deutsch, A. (eds) *Large Meteorite Impacts III*. Geological Society of America, Special Papers, **384**, 191–221.

Schulte, P., Deutsch, A., *et al*. 2009. A dual-layer Chicxulub ejecta sequence with shocked carbonate from the Cretaceous–Paleogene (K–Pg) boundary, Demerara Rise, western Atlantic. *Geochimica et Cosmochimica Acta*, **73**, 1180–1204.

Schulte, P., Alegret, L., *et al* 2010. The Chicxulub asteroid impact and mass extinction at the Cretaceous–Paleogene boundary. *Science*, **327**, 1214–1218.

Senant, J. & Popoff, M. 1991. Early Cretaceous extension in northeast Brazil related to the South Atlantic opening. *Tectonophysics*, **198**, 35–46.

Smit, J. 1999. The global stratigraphy of the Cretaceous–Tertiary boundary impact ejecta. *Annual Review of Earth and Planetary Sciences*, **27**, 75–113.

Stinnesbeck, W. & Keller, G. 1995. Comments to 'The Cretaceous–Tertiary boundary in southern low-latitude regions: Preliminary study in Pernambuco, northeastern Brazil'. *Terra Nova*, **7**, 375–382.

Stinnesbeck, W. & Keller, G. 1996. Environmental changes across the Cretaceous–Tertiary boundary in northeastern Brazil. *In*: MacLeod, N. & Keller, G. (eds) *Cretaceous–Tertiary Mass Extinctions: Biotic and Environmental Changes*. Norton, New York, 481–498.

Stinnesbeck, W. & Reyment, R.A. 1988. Note on a further occurrence of *Soudanella lacinosa* Apostolescu in northeastern Brazil. *Journal of African Earth Sciences*, **7**, 779–781.

Stinnesbeck, W., Keller, G., Adatte, T., Lopez-Oliva, J.G. & MacLeod, N. 1996. Cretaceous–Tertiary boundary clastic deposits in northeastern Mexico: impact tsunami or sea-level lowstand. *In*: MacLeod, N. & Keller, G. (eds) *Cretaceous–Tertiary Mass Extinctions: Biotic and Environmental changes*. Norton, New York, 501–547.

Ullrich, P., Berner, Z. & Kramar, U. 2011. Geochemistry of Chicxulub impact spherules in the Brazos Riverbed section, Texas, USA. *In*: Keller, G. & & Adatte, T. (eds) End-Cretaceous Mass Extinction and the Chicxulub Impact in Texas. SEPM Special Publications, **100**, 297–313.

Weaver, C.E. 1989. *Clays, Muds and Shales*. Development in Sedimentology. **44**.

Received 21 February 2012; revised typescript accepted 14 November 2012.
Scientific editing by James Hendry.